Optimal Gait Generation of an 8-DOF Biped Robot on Deformable Terrain using Floating-base Dynamics

Sunil Gora
Indian Institute of Technology, Kanpur
Kanpur, Uttar Pradesh, India
sunilg@iitk.ac.in

Shakti S. Gupta
Indian Institute of Technology, Kanpur
Kanpur, Uttar Pradesh, India
ssgupta@iitk.ac.in

Ashish Dutta
Indian Institute of Technology, Kanpur
Kanpur, Uttar Pradesh, India
adutta@iitk.ac.in

ABSTRACT

This paper presents the optimal gait generation of an 8 Degrees of Freedom (DOF) biped robot on deformable terrain. The deformation of the terrain causes the foot and terrain contact point to move during gait, and hence we have used the floating base representation for the dynamics formulation.

The foot-terrain interaction is modelled using a spring-damper model with friction constraints. The contact points acceleration changes the contact constraint resulting in change in corresponding base acceleration. Hence the contact point accelerations are obtained such that the difference of the actual and desired base acceleration is minimized. The base acceleration is obtained using contact forces due to foot contact with the terrain and the contact point acceleration. The corresponding joint torques are obtained using equations of motion of the biped. The variation of the hip trajectory with the coefficient of friction of the terrain and deformation of the terrain has been analysed. The variation of the required coefficient of friction and center of pressure are also analyzed in this paper. The results show that the error in the hip trajectory between the desired and actual trajectory, depends on the coefficient of friction and deformation of the terrain. The results are useful in determining the terrain conditions on which the robot can walk stably.

CCS CONCEPTS

• **Computer systems organization → Robotics**; *Robotic autonomy*; *Robotic components.*

KEYWORDS

Biped Robot, Gait Generation, Contact Dynamics

ACM Reference Format:
Sunil Gora, Shakti S. Gupta, and Ashish Dutta. 2021. Optimal Gait Generation of an 8-DOF Biped Robot on Deformable Terrain using Floating-base Dynamics. In *Advances in Robotics - 5th International Conference of The Robotics Society (AIR2021), June 30-July 4, 2021, Kanpur, India.* ACM, New York, NY, USA, 6 pages. https://doi.org/10.1145/3478586.3478640

AIR2021, June 30-July 4, 2021, Kanpur, India

ACM ISBN 978-1-4503-8971-6/21/06…$15.00
https://doi.org/10.1145/3478586.3478640

1 INTRODUCTION

Legged locomotion is one of the active areas of research in robotics. The aspects of dynamic balancing [6, 12, 14, 22], gait generation [2, 8, 11, 18], and control [7, 15, 21] have significant contributions in walking of legged robots. The Zero Moment Point (ZMP) [22], which is the point at which the moment of gravity and inertia forces is zero, is widely used for stable walking on flat hard terrain with sufficient friction. The concentrated mass model such as Center of Mass (COM)-ZMP Model is used for motion control [11]. Using Linear Inverted Pendulum Mode [9], the robot dynamics is linearized for control [8] and stabilization [14]. Virtual ZMP and contact plane is used in virtual slope method [18] for walking on stairs. Nonlinear Inverted Pendulum (NIP) walking over uneven terrain is demonstrated using foot placement method, based on the total energy of the system [2]. In [6], stability criterion is presented for the contact forces acting due to foot contact with the environment. Contact Wrench Cone [1] conditions are demonstrated for contact stability. Trajectory generation using genetic algorithm and energy optimal walking [20] is achieved by the correction of deformation of the sole of the foot. In [24], the compliant contact model approach is shown for stable walking on soft ground with small deformation. The foot-soil interaction model and parameter estimation with experimental setup using cylindrical foot of quadruped robot is presented in [3].

On the other hand, the floating-base model dynamics and control of the legged robots has also been explored by many researchers [10, 13, 19]. In [13], a general framework for dynamics using virtual joints and the operation space control for different contact states is proposed. Inverse dynamics control independent of external constraint forces is achieved in [10]. In [19], dynamics formulation using Decoupled Natural Orthogonal Complement (DeNOC) matrices and model-based controller is presented. An Inverse dynamics controller for optimized contact force distribution is proposed in [16]. Soft Terrain Adaptation and Compliance Estimation (STANCE) [4] is developed for whole body control and terrain compliance estimation and implemented on a quadruped robot walking over different types of terrain. The effect of contact forces obtained by foot-terrain interaction model on floating-base model and the analysis of variation of terrain parameters for biped robot is not reported in the literature and is the main objective of this paper.

2 KINEMATICS OF 8-DOF BIPED ROBOT

The biped robot can be represented as fixed-base or floating-base model. In fixed-base representation, the contact point is considered as fixed reference frame, and the change of contact points also requires the change of model representation. The floating-base model is a general representation of any multi-body system moving freely. The moving reference frame has 6 Degrees of Freedom (DOF), three rotational and three translational, and can incorporate the changing contact states. On deformable terrain, the contact point is also having acceleration, and floating-base model is used to provide the 6 degrees of freedom to the contact points. The base reference frame is attached to the center of mass of hip link, which moves freely with respect to the inertial frame as shown in Fig. 1. The generalized joint coordinates can be written as,

$$\boldsymbol{q} = \begin{bmatrix} \boldsymbol{q}_0 \\ \boldsymbol{q}_\theta \end{bmatrix}. \tag{1}$$

Here, $\boldsymbol{q}_0 \in \boldsymbol{R}^{6\times1}$ is the vector of position and orientation of base reference frame in inertial frame represented by virtual degrees of freedom, denoted by (x_0, y_0, z_0) and $(\theta_{x0}, \theta_{y0}, \theta_{z0})$, respectively. $\boldsymbol{q}_\theta \in \boldsymbol{R}^{n\times1}$ is the vector of actuated joint coordinates of the robot. The angular and linear velocities of the stance leg and swing leg ankle is given by

$$\begin{bmatrix} \dot{\boldsymbol{o}}_{st} \\ \dot{\boldsymbol{o}}_{sw} \end{bmatrix} = \boldsymbol{J}_0\dot{\boldsymbol{q}}_0 + \boldsymbol{J}_\theta\dot{\boldsymbol{q}}_\theta, \tag{2}$$

where, $\boldsymbol{J}_0 = \begin{bmatrix} \boldsymbol{J}_{0_{st}} \\ \boldsymbol{J}_{0_{sw}} \end{bmatrix} \in \boldsymbol{R}^{12\times6}$, and $\boldsymbol{J}_\theta = \begin{bmatrix} \boldsymbol{J}_{\theta_{st}} \\ \boldsymbol{J}_{\theta_{sw}} \end{bmatrix} \in \boldsymbol{R}^{12\times n}$, are the corresponding jacobian matrices.

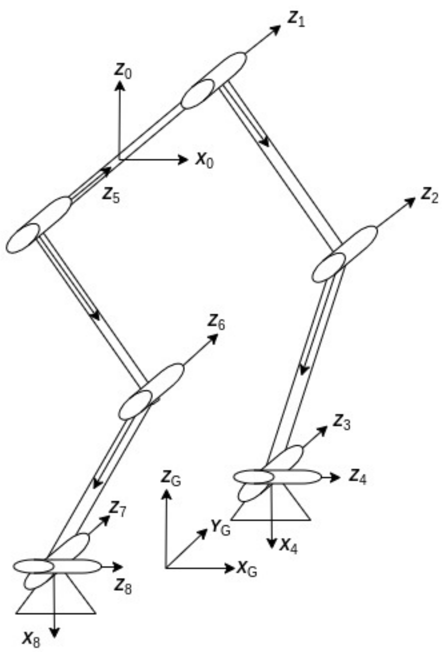

Figure 1: Floating base representation

2.1 Trajectory generation

The position of stance leg ankle, $\boldsymbol{o}_{st}$ given the position of hip link center (x_0, y_0, z_0) is written as

$$\boldsymbol{o}_{st} = \begin{bmatrix} x_0 \\ y_0 \\ z_0 \end{bmatrix} - \begin{bmatrix} H_x \\ H_y \\ H_z \end{bmatrix}. \tag{3}$$

Here, (H_x, H_y, H_z) is the position of the hip link center with respect to stance leg ankle. The trajectory of hip center with respect to stance ankle [17] in the X direction, H_x is given as

$$H_x = a_0 + a_1 t + a_2 t^2 + a_3 t^3. \tag{4}$$

The sinusoidal trajectory is used for hip center with respect to stance ankle in the Z direction, H_z with average hip height H_{z_0}, amplitude a_{H_z} and step time t_c as

$$H_z = H_{z_0} - a_{H_z}\sin(2\pi t/t_c). \tag{5}$$

The position of hip center with respect to stance ankle in Y direction, H_y is obtained using the tilt angle of the robot in coronal plane. The cubic polynomial trajectory for the tilt angle, θ_{tilt} is

$$\theta_{tilt} = b_0 + b_1 t + b_2 t^2 + b_3 t^3. \tag{6}$$

Spline trajectories are used in X and Z directions for the swing leg as

$$x_{sw} = c_0 + c_1 t + c_2 t^2 + c_3 t^3, \tag{7}$$

$$z_{sw} = d_0 + d_1 t + d_2 t^2 + d_3 t^3. \tag{8}$$

The constants a_i, b_i, c_i and d_i are obtained given the initial and final positions and velocities of the robot. The corresponding joint angles for the given trajectories are obtained using inverse kinematics [17].

3 DYNAMICS OF FLOATING-BASE ROBOT

The equations of motion of the floating-base robot are written as

$$\begin{bmatrix} \boldsymbol{I}_0 & \boldsymbol{I}_{0\theta} \\ \boldsymbol{I}_{0\theta}^T & \boldsymbol{I}_\theta \end{bmatrix} \begin{bmatrix} \ddot{\boldsymbol{q}}_0 \\ \ddot{\boldsymbol{q}}_\theta \end{bmatrix} + \begin{bmatrix} \boldsymbol{c}_0 \\ \boldsymbol{c}_\theta \end{bmatrix} = \begin{bmatrix} \boldsymbol{0} \\ \boldsymbol{\tau}_\theta \end{bmatrix} + \begin{bmatrix} \boldsymbol{J}_{c_0}^T \\ \boldsymbol{J}_{c_\theta}^T \end{bmatrix} \boldsymbol{w}_c, \tag{9}$$

where, $\boldsymbol{I}_0 \in \boldsymbol{R}^{6\times6}$ and $\boldsymbol{I}_\theta \in \boldsymbol{R}^{n\times n}$ are inertia matrices of the hip link and legs, respectively, $\boldsymbol{I}_{0\theta} \in \boldsymbol{R}^{6\times n}$ is the coupling inertia matrix, $\boldsymbol{c}_0 \in \boldsymbol{R}^{6\times1}$ and $\boldsymbol{c}_\theta \in \boldsymbol{R}^{n\times1}$ are the position and velocity dependent nonlinear terms associated with the hip link and legs, respectively, $\boldsymbol{\tau}_\theta \in \boldsymbol{R}^{n\times1}$ is the vector of joint torques, $\boldsymbol{J}_{c_0} \in \boldsymbol{R}^{6c\times6}$ and $\boldsymbol{J}_{c_\theta} \in \boldsymbol{R}^{6c\times n}$ are jacobian matrices for the hip link and legs, respectively, $\boldsymbol{w}_c = \begin{bmatrix} \boldsymbol{w}_{st}^T & \boldsymbol{w}_{sw}^T \end{bmatrix}^T \in \boldsymbol{R}^{12\times1}$ is the wrench vector of moments and forces acting at the stance and swing leg ankles due to contact forces and jacobian matrices are also obtained according to the contact states.

3.1 Floating-base Dynamics

The equations of motion of the floating base is written from Eq. (9) as

$$\boldsymbol{I}_0\ddot{\boldsymbol{q}}_0 + \boldsymbol{I}_{0\theta}\ddot{\boldsymbol{q}}_\theta + \boldsymbol{c}_0 = \boldsymbol{J}_{c_0}^T\boldsymbol{w}_c. \tag{10}$$

The external force on the robot is due to the contact of the legs with the environment [10]. Considering the compliant contact having angular and linear acceleration of contact leg ankle denoted by $\ddot{\boldsymbol{o}}_c = \begin{bmatrix} \ddot{\boldsymbol{o}}_{st}^T & \ddot{\boldsymbol{o}}_{sw}^T \end{bmatrix}^T \in \boldsymbol{R}^{12\times1}$, the contact constraint using Eq. (2) is given as

$$\boldsymbol{J}_{c_0}\ddot{\boldsymbol{q}}_0 + \dot{\boldsymbol{J}}_{c_0}\dot{\boldsymbol{q}}_0 + \boldsymbol{J}_{c_\theta}\ddot{\boldsymbol{q}}_\theta + \dot{\boldsymbol{J}}_{c_\theta}\dot{\boldsymbol{q}}_\theta = \ddot{\boldsymbol{o}}_c. \tag{11}$$

By combining Eqs. (10) and (11), we obtain

$$\begin{bmatrix} \boldsymbol{I}_0 \\ \boldsymbol{J}_{c_0} \end{bmatrix} \ddot{\boldsymbol{q}}_0 + \begin{bmatrix} \boldsymbol{I}_{0\theta} \\ \boldsymbol{J}_{c_\theta} \end{bmatrix} \ddot{\boldsymbol{q}}_\theta + \begin{bmatrix} \boldsymbol{c}_0 \\ \dot{\boldsymbol{J}}_{c_0}\dot{\boldsymbol{q}}_0 + \dot{\boldsymbol{J}}_{c_\theta}\dot{\boldsymbol{q}}_\theta \end{bmatrix} = \begin{bmatrix} \boldsymbol{J}_{c_0}^T\boldsymbol{w}_c \\ \ddot{\boldsymbol{o}}_c \end{bmatrix}. \tag{12}$$

In inverse dynamics, the acceleration of base frame and the joint torques are obtained for a desired trajectory. The floating base acceleration and required contact wrench is obtained by solving the equation given as

$$\begin{bmatrix} \boldsymbol{I}_0 & -\boldsymbol{J}_{c_0}^T \\ \boldsymbol{J}_{c_0} & \boldsymbol{0} \end{bmatrix} \begin{bmatrix} \ddot{\boldsymbol{q}}_0 \\ \boldsymbol{w}_c \end{bmatrix} = \begin{bmatrix} -\boldsymbol{I}_{0\theta}\ddot{\boldsymbol{q}}_\theta - \boldsymbol{c}_0 \\ \ddot{\boldsymbol{o}}_c - \boldsymbol{J}_{c\theta}\ddot{\boldsymbol{q}}_\theta - \dot{\boldsymbol{J}}_{c_0}\dot{\boldsymbol{q}}_0 - \dot{\boldsymbol{J}}_{c\theta}\dot{\boldsymbol{q}}_\theta \end{bmatrix}. \quad (13)$$

Next, the joint torques are obtained by,

$$\boldsymbol{\tau}_\theta = \boldsymbol{I}_{0\theta}^T\ddot{\boldsymbol{q}}_0 + \boldsymbol{I}_\theta\ddot{\boldsymbol{q}}_\theta + \boldsymbol{c}_\theta - \boldsymbol{J}_{c\theta}^T\boldsymbol{w}_c. \quad (14)$$

In inverse dynamics problem, the required contact force obtained from Eq. (13) should be inside the contact wrench cone, but the actual contact forces exerted on robot due to contact are always inside the contact wrench cone. So, the stable gait can be generated given the actual contact forces. Using the motion of the floating-base obtained for a desired trajectory from Eq. (10) in Eq. (11), we get

$$\ddot{\boldsymbol{o}}_c = \boldsymbol{J}_{c_0}\boldsymbol{I}_0^{-1}(\boldsymbol{J}_{c_0}^T\boldsymbol{w}_c - \boldsymbol{I}_{0\theta}\ddot{\boldsymbol{q}}_{\theta_{desired}} - \boldsymbol{c}_0) + \dot{\boldsymbol{J}}_{c_0}\dot{\boldsymbol{q}}_0 + \boldsymbol{J}_{c\theta}\ddot{\boldsymbol{q}}_{\theta_{desired}} + \dot{\boldsymbol{J}}_{c\theta}\dot{\boldsymbol{q}}_{\boldsymbol{\theta}}. \quad (15)$$

Next, the optimal joint accelerations are obtained using the above equation and the desired floating-base acceleration with the joint constraints as

$$\ddot{\boldsymbol{q}}_{\boldsymbol{\theta}} = \boldsymbol{J}_{c\theta}^+(\ddot{\boldsymbol{o}}_c - \boldsymbol{J}_{c_0}\ddot{\boldsymbol{q}}_{0_{desired}} - \dot{\boldsymbol{J}}_{c_0}\dot{\boldsymbol{q}}_0 - \dot{\boldsymbol{J}}_{c\theta}\dot{\boldsymbol{q}}_\theta). \quad (16)$$

Finally, the base motion is obtained using Eq. (10) and corresponding joint torques are obtained using Eq. (14).

3.2 Foot-terrain Interaction Model

The external contact forces obtained from foot-terrain interaction model will generate a stable gait trajectory. The contact force at any contact point can be written as

$$\boldsymbol{f}_c = \begin{bmatrix} f_x \\ f_y \\ f_n \end{bmatrix}. \quad (17)$$

Here, the contact force component, f_n is obtained by summation of the contact forces of normal contact model, i.e., $f_n = \sum f_{n_i}$. Considering the spring-damper contact model [5] with stiffness k_n, and damping coefficient c_n, at the contact point (x_i, y_i, z_i), the normal contact force f_{n_i} is given by

$$f_{n_i} = \begin{cases} k_n z_i + c_n \dot{z}_i, & z_i < 0, \\ 0, & z_i \geq 0. \end{cases} \quad (18)$$

The Center of Pressure (CoP) for the flat rectangular foot is obtained by

$$x_{CoP} = \frac{\sum f_{n_i} x_i}{f_n}, \qquad y_{CoP} = \frac{\sum f_{n_i} y_i}{f_n}. \quad (19)$$

The tangential spring-damper model with stiffness k_t, and damping coefficient c_t, gives,

$$\boldsymbol{f}_t = \begin{cases} k_t\delta_t + c_t\dot{\delta}_t, & |\boldsymbol{f}_t| \leq \mu f_n, \\ \pm\mu\boldsymbol{f}_n, & |\boldsymbol{f}_t| > \mu f_n. \end{cases} \quad (20)$$

The required coefficient of friction from tangential contact model is

$$\mu_{req} = \frac{f_t}{f_n}. \quad (21)$$

4 RESULTS AND DISCUSSION

Biped robot with 8-DOF is used for inverse dynamics. The design parameters of the robot [17] and terrain parameters [23] for the simulation are shown in Table 1. The inverse dynamics simulation time is 3.201 seconds for the motion time 1 second with time interval 0.0067 seconds in MATLAB using Intel core i5-4460 3.20GHz processor. The inverse dynamics results are obtained starting with left leg as stance leg, which stays in contact with the terrain, and right leg as swing leg, which moves forward by the distance called step length. In following step, the right leg becomes stance leg and left leg becomes swing leg. The desired hip trajectory is obtained using Eq. (3), where the stance leg ankle position in vertical direction is modified based on the ground deformation. The joint angles are obtained using inverse kinematics.

Table 1: Parameters for robot simulation

Total mass m	0.9516 kg
Thigh length L_1	111 mm
Shank length L_2	111 mm
Lower-trunk length L_h	42.5 mm
Height of ankle from grounded foot L_{ah}	32 mm
Foot size	60 mm x 60 mm
Step length	120 mm
Normal spring constant k_n	10 kN/m
Tangential spring constant k_t	1 kN/m
Normal damping coefficient c_n	50 N-s/m
Tangential damping coefficient c_t	50 N-s/m
Friction coefficient	0.5
Step time	1.5 s
Number of steps	2
Maximum tilt angle	8^o
Maximum height of swing leg	30 mm
Amplitude of hip sinusoidal trajectory	5 mm
Initial position of floating base hip link (in m)	(0, 0, 0.2207)
Initial joint angles of stance leg θ_{1-4} (in rad)	0.8789, 1.0684, -0.3812, 0
Final joint angles of stance leg θ_{1-4} (in rad)	1.1943, 1.0684 -0.7209, 0
Initial joint angles of swing leg θ_{5-8} (in rad)	1.1943, 1.0684, -0.6965, 0
Final joint angles of swing leg θ_{5-8} (in rad)	0.8789, 1.0684, -0.4055, 0

The simulation of walking gait generated for two steps is shown in Fig. 2. The trajectories of hip link center, stance and swing leg ankles are also shown. The motion of stance leg foot due to deformation of the terrain is also evident in the figure.

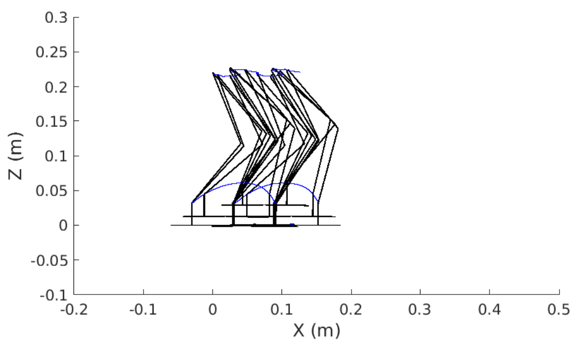

Figure 2: Multi-step simulation of the Biped on deformable terrain

The flat rectangular feet with four contact points at the edges is considered, and the contact forces are obtained using contact model. The reaction forces and moments at the ankle are obtained by the summation of forces at the contact edges and the summation of moments about ankle. The reaction forces and moments acting at the ankle in reference frame attached at the foot are shown in Fig. 3.

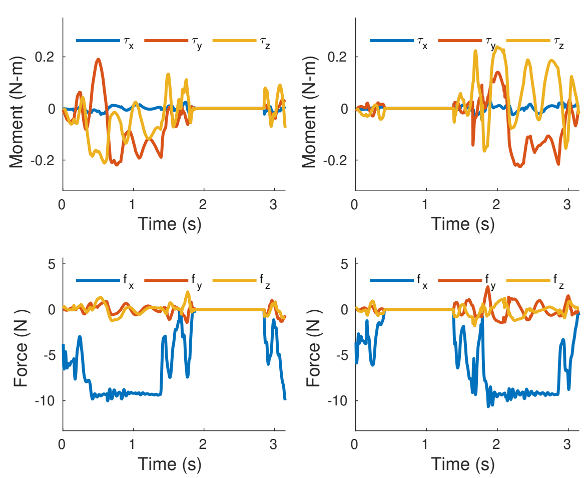

Figure 3: Reaction forces and moments at ankles of left leg and right leg

The center of pressure of normal reaction force acting on the stance leg and swing leg is obtained using Eq. (19) and shown in Fig. 4. The center of pressure of total reaction force on the robot is also shown, which coincides with CoP of the stance leg in single support phase.

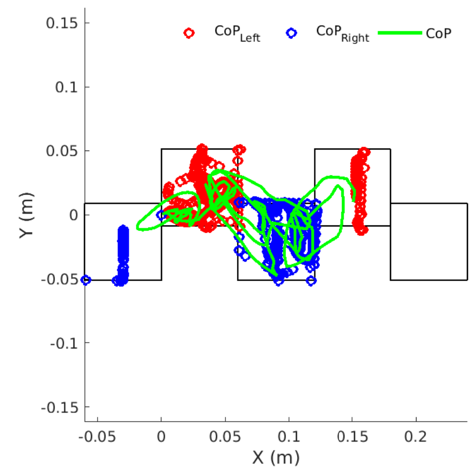

Figure 4: Center of pressure

In Fig. 5, the required coefficient of friction, i.e., the ratio of tangential force to the normal force for the stance leg and swing leg is shown over the period of time. In this case, the required friction coefficient reaches coefficient of friction of the terrain only when the normal reaction force reduces to zero.

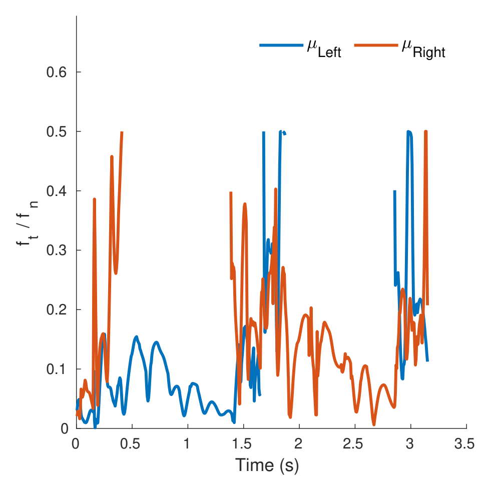

Figure 5: Required Coefficient of friction

The ankle trajectories, i.e., the position, velocity and acceleration of the stance leg and swing leg are shown in Fig. 6. The motion of stance leg ankle in Z direction changes the normal component, and in the plane of terrain changes the tangential component of the reaction force.

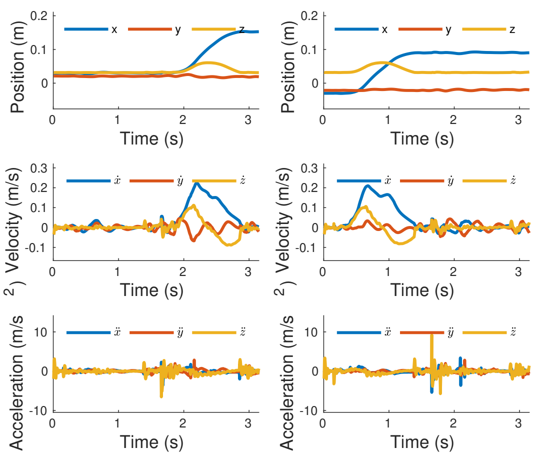

Figure 6: Ankle trajectories of the left and right leg

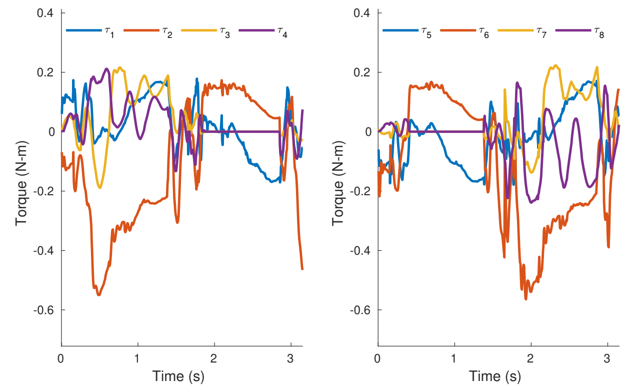

Figure 8: Joint torques of left (τ_{1-4})and right (τ_{5-8}) leg

The desired and actual trajectory of the center of hip link are shown in Fig. 7. The hip trajectory in Z-direction is corrected based on the deformation of the terrain. The variation in trajectory is due to the rotation of the foot and deformation of the terrain in tangential direction as the coefficient of friction is sufficient for the robot motion.

Stable walking gait is also generated for $k_n = 100kN/m$, $k_t = 10kN/m$, $c_n = c_t = 100Ns/m$, and $\mu = 0.2$. The variation of center of pressure due to change of foot position and orientation, and the required coefficient of friction are shown in Fig. 9 and 10, respectively. The fluctuations of required coefficient of friction in the figure shows the sensitivity of the contact model.

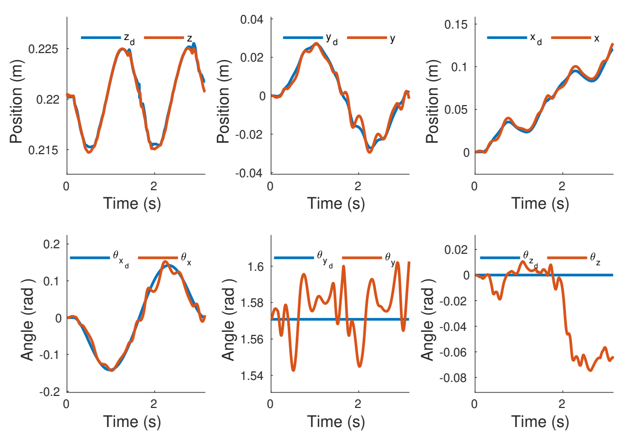

Figure 7: Desired and actual hip trajectory

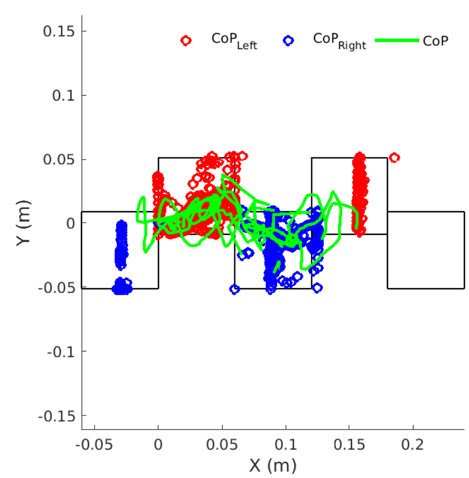

Figure 9: Center of pressure for $k_n = 100kN/m$, $k_t = 10kN/m$, $c_n = 100Ns/m$, $c_t = 100Ns/m$, and $\mu = 0.2$

In Fig. 8, the joint torques obtained for the stance leg and swing leg are shown. The joint torque profiles have the symmetry of leg phases and are useful to generate cyclic trajectory for walking.

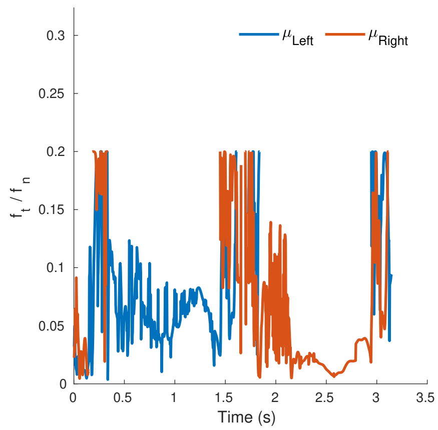

Figure 10: Required coefficient of friction for $k_n = 100kN/m$, $k_t = 10kN/m$, $c_n = 100Ns/m$, $c_t = 100Ns/m$, and $\mu = 0.2$

5 CONCLUSION

In this paper, the dynamics formulation and optimal trajectory generation of an 8 DOF biped robot on deformable terrain is presented. The motion of floating base due to contact forces obtained from normal and tangential contact model and contact point acceleration were found. The error in trajectory of hip link center due to deformation of the terrain and coefficient of friction is also presented. The ankle motion, variation of center of pressure and required coefficient of friction of the stance leg and swing leg was analysed. The results show the effect of the coefficient of friction on the hip trajectory. Also, the minimum friction required for walking with different terrain parameters was obtained for the 8 DOF biped robot.

REFERENCES

[1] Stéphane Caron, Quang-Cuong Pham, and Yoshihiko Nakamura. 2015. Stability of surface contacts for humanoid robots: Closed-form formulae of the contact wrench cone for rectangular support areas. In *2015 IEEE International Conference on Robotics and Automation (ICRA)*. IEEE, 5107–5112.

[2] Steven Crews and Matthew Travers. 2020. Energy Management Through Footstep Selection For Bipedal Robots. *IEEE Robotics and Automation Letters* 5, 4 (2020), 5485–5493.

[3] Liang Ding, Haibo Gao, Zongquan Deng, Jianhu Song, Yiqun Liu, Guangjun Liu, and Karl Iagnemma. 2013. Foot–terrain interaction mechanics for legged robots: Modeling and experimental validation. *The International Journal of Robotics Research* 32, 13 (2013), 1585–1606.

[4] Shamel Fahmi, Michele Focchi, Andreea Radulescu, Geoff Fink, Victor Barasuol, and Claudio Semini. 2020. Stance: Locomotion adaptation over soft terrain. *IEEE Transactions on Robotics* 36, 2 (2020), 443–457.

[5] Gianni Gilardi and Inna Sharf. 2002. Literature survey of contact dynamics modelling. *Mechanism and machine theory* 37, 10 (2002), 1213–1239.

[6] Hirohisa Hirukawa, Shizuko Hattori, Kensuke Harada, Shuuji Kajita, Kenji Kaneko, Fumio Kanehiro, Kiyoshi Fujiwara, and Mitsuharu Morisawa. 2006. A universal stability criterion of the foot contact of legged robots-adios zmp. In *Proceedings 2006 IEEE International Conference on Robotics and Automation, 2006. ICRA 2006.* IEEE, 1976–1983.

[7] Shuuji Kajita, Fumio Kanehiro, Kenji Kaneko, Kiyoshi Fujiwara, Kensuke Harada, Kazuhito Yokoi, and Hirohisa Hirukawa. 2003. Biped walking pattern generation by using preview control of zero-moment point. In *2003 IEEE International Conference on Robotics and Automation (Cat. No. 03CH37422)*, Vol. 2. IEEE, 1620–1626.

[8] Shuuji Kajita, Fumio Kanehiro, Kenji Kaneko, Kazuhito Yokoi, and Hirohisa Hirukawa. 2001. The 3D linear inverted pendulum mode: A simple modeling for a biped walking pattern generation. In *Proceedings 2001 IEEE/RSJ International Conference on Intelligent Robots and Systems. Expanding the Societal Role of Robotics in the the Next Millennium (Cat. No. 01CH37180)*, Vol. 1. IEEE, 239–246.

[9] Shuuji Kajita and Kazuo Tani. 1991. Study of dynamic biped locomotion on rugged terrain-derivation and application of the linear inverted pendulum mode. In *Proceedings. 1991 IEEE International Conference on Robotics and Automation.* IEEE Computer Society, 1405–1406.

[10] Michael Mistry, Jonas Buchli, and Stefan Schaal. 2010. Inverse dynamics control of floating base systems using orthogonal decomposition. In *2010 IEEE international conference on robotics and automation.* IEEE, 3406–3412.

[11] Kazuhisa Mitobe, Genci Capi, and Yasuo Nasu. 2000. Control of walking robots based on manipulation of the zero moment point. *Robotica* 18, 6 (2000), 651–657.

[12] David E Orin, Ambarish Goswami, and Sung-Hee Lee. 2013. Centroidal dynamics of a humanoid robot. *Autonomous robots* 35, 2 (2013), 161–176.

[13] Jaeheung Park and Oussama Khatib. 2006. Contact consistent control framework for humanoid robots. In *Proceedings 2006 IEEE International Conference on Robotics and Automation, 2006. ICRA 2006.* IEEE, 1963–1969.

[14] Jerry Pratt, John Carff, Sergey Drakunov, and Ambarish Goswami. 2006. Capture point: A step toward humanoid push recovery. In *2006 6th IEEE-RAS international conference on humanoid robots.* IEEE, 200–207.

[15] Jerry Pratt, Chee-Meng Chew, Ann Torres, Peter Dilworth, and Gill Pratt. 2001. Virtual model control: An intuitive approach for bipedal locomotion. *The International Journal of Robotics Research* 20, 2 (2001), 129–143.

[16] Ludovic Righetti, Jonas Buchli, Michael Mistry, Mrinal Kalakrishnan, and Stefan Schaal. 2013. Optimal distribution of contact forces with inverse-dynamics control. *The International Journal of Robotics Research* 32, 3 (2013), 280–298.

[17] Abhishek Sarkar and Ashish Dutta. 2015. 8-DoF biped robot with compliant-links. *Robotics and Autonomous Systems* 63 (2015), 57–67.

[18] Tomoya Sato, Sho Sakaino, Eijiro Ohashi, and Kouhei Ohnishi. 2010. Walking trajectory planning on stairs using virtual slope for biped robots. *IEEE transactions on industrial electronics* 58, 4 (2010), 1385–1396.

[19] Suril Vijaykumar Shah, Subir Kumar Saha, and Jayanta Kumar Dutt. 2013. Dynamics of tree-type robotic systems. In *Dynamics of Tree-Type Robotic Systems.* Springer, 73–88.

[20] Maitray Shrivastava, Ashish Dutta, and Anupam Saxena. 2007. Trajectory generation using GA for an 8 DOF biped robot with deformation at the sole of the foot. *Journal of Intelligent and Robotic Systems* 49, 1 (2007), 67–84.

[21] Tomomichi Sugihara, Yoshihiko Nakamura, and Hirochika Inoue. 2002. Real-time humanoid motion generation through ZMP manipulation based on inverted pendulum control. In *Proceedings 2002 IEEE International Conference on Robotics and Automation (Cat. No. 02CH37292)*, Vol. 2. IEEE, 1404–1409.

[22] Miomir Vukobratović and Branislav Borovac. 2004. Zero-moment point—thirty five years of its life. *International journal of humanoid robotics* 1, 01 (2004), 157–173.

[23] Jo Yung Wong et al. 1989. *Terramechanics and off-road vehicles.* Elsevier.

[24] Yuan F Zheng, Hongfei Wang, Shimeng Li, Yiping Liu, D Orin, Kiwon Sohn, Youngbum Jun, and Paul Oh. 2013. Humanoid robots walking on grass, sands and rocks. In *2013 IEEE Conference on Technologies for Practical Robot Applications (TePRA).* IEEE, 1–6.